

## First 3D 3d–4f Interpenetrating Structure: Synthesis, Reaction, and Characterization of $\{[\text{LnCr}(\text{IDA})_2(\text{C}_2\text{O}_4)]\}_n$

Bin Zhai, Long Yi, Hong-Shen Wang, Bin Zhao, Peng Cheng,\* Dai-Zheng Liao, and Shi-Ping Yan

Department of Chemistry, Nankai University, Tianjin 300071, People's Republic of China

Received May 9, 2006

The hydrothermal reaction of  $\text{Cr}(\text{NO}_3)_3$ ,  $\text{Ln}_2\text{O}_3$ , and iminodiacetic acid ( $\text{H}_2\text{IDA}$ ) in the molar ratio of 1:1:3 produced  $\{[\text{LnCr}(\text{IDA})_2(\text{C}_2\text{O}_4)]\}_n$  ( $\text{Ln} = \text{Eu}$ , **1**;  $\text{Sm}$ , **2**), which represent the first 3D 3d–4f interpenetrating coordination polymers. In the reaction, the  $\text{H}_2\text{IDA}$  ligands partly decompose into oxalate anions (ox), which connect  $\text{Ln}^{\text{III}}$  ions to form 1D  $\{\text{Ln}(\text{ox})\}_n$  chains. Each of the  $\text{Cr}^{\text{III}}$  ions is tridentate-coordinated by two IDA ligands, which act as tetradentate metalloligands to link  $\{\text{Ln}(\text{ox})\}_n$  chains to form 3D open networks. The two open networks interpenetrate each other to form nonporous products. **1** and **2** are thermally stable up to 327 and 360 °C, respectively. Both of complexes show normally paramagnetic behavior. The luminescent results imply that the energy transfers from  $\text{Ln}^{\text{III}}$  to  $\text{Cr}^{\text{III}}$  are strong.

The construction of three-dimensional (3D) coordination polymers has been a field of rapid growth in supramolecular and material chemistry because of the formation of fascinating structures and their potentially useful ion-exchange, adsorption, catalytic, fluorescence, and magnetic properties.<sup>1</sup> Consequently, a variety of 3D metal–organic frameworks (MOFs) have been prepared through taking certain factors into account, such as the coordination nature of the metal ion, as well as the shape, functionality, flexibility, and symmetry of organic ligands.<sup>2</sup> Multicarboxylate ligands are frequently chosen to construct a 3D MOF because of their rich coordination modes.<sup>3</sup> For example, a series of carboxylate–zinc 3D MOFs with remarkable

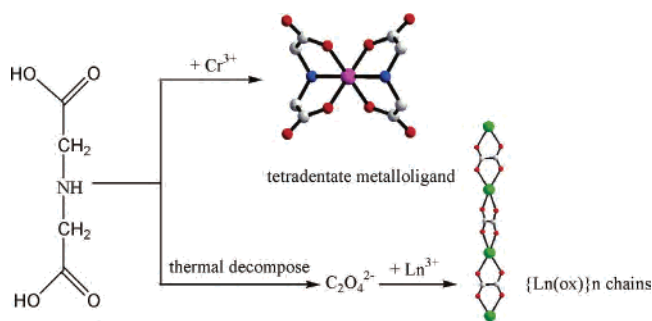
methane- and hydrogen-storage properties have been prepared by some groups.<sup>4</sup> However, the syntheses of 3D MOFs have so far been exclusively centered on monometallic 3D coordination polymers,<sup>1–4</sup> while the chemistry, as well as the synthetic strategy toward heterometallic coordination polymers, especially for these complexes containing rare-earth ions, has received much less attention<sup>5</sup> because of the variable and versatile coordination behavior of 4f metal ions. For example, there are only a few examples for discrete molecules<sup>6</sup> and even fewer examples for coordination polymers<sup>7</sup> of  $\text{Ln}^{\text{III}}\text{–Cr}^{\text{III}}$  complexes.

We have developed a series of 3D  $\text{Ln}\text{–Mn}$  zeolite-type nanoporous materials under hydrothermal conditions based on pyridine-2,6-dicarboxylic acid,<sup>5a</sup> and their luminescent properties were further investigated.<sup>8</sup> Very recently, we

\* To whom correspondence should be addressed. E-mail: pcheng@nankai.edu.cn. Fax: +86-22-23502458.

- (1) (a) Moulton, B.; Zaworotko, M. J. *Chem. Rev.* **2001**, *101*, 1629. (b) Evans, O. R.; Lin, W. B. *Acc. Chem. Res.* **2002**, *35*, 511. (c) Kil, S. M.; Myunghyun, P. S. *J. Am. Chem. Soc.* **2000**, *122*, 6834. (d) Fujita, M.; Oka, H.; Yamaguchi, K.; Ogura, K. *Nature (London)* **1995**, *378*, 469.
- (2) (a) Reger, D. L.; Wright, T. D.; Semeniuc, R. F.; Grattan, T. C.; Smith, M. D. *Inorg. Chem.* **2001**, *40*, 6212. (b) Zaman, M. B.; Smith, M. D.; zur Loye, H. C. *Chem. Commun.* **2001**, 2256. (c) Kitaura, R.; Seki, K.; Akiyama, G.; Kitagawa, S. *Angew. Chem., Int. Ed.* **2003**, *42*, 428. (d) Kitaura, R.; Fujimoto, K.; Noro, S.; Kondo, M.; Kitagawa, S. *Angew. Chem., Int. Ed.* **2002**, *41*, 133. (e) Yi, L.; Ding, B.; Zhao, B.; Cheng, P.; Liao, D.-Z.; Yan, S.-P.; Jiang, Z.-H. *Inorg. Chem.* **2004**, *43*, 33. (f) Heintz, R. A.; Zhao, H.; Ouyang, X.; Grandinetti, G.; Cowen, J.; Dumbor, K. R. *Inorg. Chem.* **1999**, *38*, 144.

- (3) (a) Prior, T. J.; Bradshaw, D.; Teat, S. J.; Rosseinsky, M. J. *Chem. Commun.* **2003**, 500. (b) Bourne, S. A.; Lu, J. J.; Mondal, A.; Moulton, B.; Zaworotko, M. J. *Angew. Chem., Int. Ed.* **2001**, *40*, 2111. (c) Lu, J. J.; Mondal, A.; Moulton, B.; Zaworotko, M. J. *Angew. Chem., Int. Ed.* **2001**, *40*, 2113. (d) Ding, B.; Yi, L.; Liu, Y.; Cheng, P.; Dong, Y.-B.; Ma, J.-P. *Inorg. Chem. Commun.* **2005**, *8*, 38. (e) Zhao, B.; Yi, L.; Dai, Y.; Chen, X.-Y.; Cheng, P.; Liao, D.-Z.; Yan, S.-P.; Jiang, Z.-H. *Inorg. Chem.* **2005**, *44*, 911.
- (4) (a) Eddaoudi, M.; Kim, J.; Rosi, N.; Vodak, D.; Wachter, J.; O'Keeffe, M.; Yaghi, O. M. *Science* **2002**, *295*, 469. (b) Rosi, N. L.; Eckert, J.; Eddaoudi, M.; Vodak, D. T.; Kim, J.; O'Keeffe, M.; Yaghi, O. M. *Science* **2003**, *300*, 1127. (c) Chae, H. K.; Siberio-Perez, D. Y.; Kim, J.; Go, Y.; Eddaoudi, M.; Matzger, A. J.; O'Keeffe, M.; Yaghi, O. M. *Nature (London)* **2004**, *427*, 523.
- (5) (a) Zhao, B.; Cheng, P.; Dai, Y.; Cheng, C.; Liao, D. Z.; Yan, S. P.; Jiang, Z. H.; Wang, G. L. *Angew. Chem., Int. Ed.* **2003**, *42*, 934. (b) Ren, Y. P.; Long, L. S.; Mao, B. W.; Yuan, Y. Z.; Huang, R. B.; Zheng, L. S. *Angew. Chem., Int. Ed.* **2003**, *42*, 532. (c) Imaz, I.; Bravic, G.; Sutter, J.-P. *Chem. Commun.* **2005**, 993. (d) Gheorghe, R.; Cucos, P.; Andruh, M.; Costes, J.-P.; Donnadieu, B.; Shova, S. *Chem.–Eur. J.* **2006**, *12*, 187.
- (6) (a) Torelli, S.; Imbert, D.; Cantuel, M.; Bernardinelli, G.; Delahaye, S.; Hauser, A.; Bünzli, J.-C. G.; Piguët, C. *Chem.–Eur. J.* **2005**, *11*, 3228. (b) Subhan, M. S.; Suzuki, T.; Kaizaki, S. *J. Chem. Soc., Dalton Trans.* **2001**, 492. (c) Cantuel, M.; Bernardinelli, G.; Imbert, D.; Bünzli, J.-C. G.; Hopfgartner, G.; Piguët, C. *J. Chem. Soc., Dalton Trans.* **2002**, 1929. (d) Sanada, T.; Suzuki, T.; Yoshida, T.; Kaizaki, S. *Inorg. Chem.* **1998**, *37*, 4712. (e) Akitsu, T.; Einaga, Y. *Inorg. Chim. Acta* **2006**, *359*, 1421.
- (7) (a) Decurtins, S.; Gross, M.; Schmale, H. W.; Ferlay, S. *Inorg. Chem.* **1998**, *37*, 2443. (b) Kou, H.-Z.; Zhou, B. C.; Gao, S.; Wang, R.-J. *Angew. Chem., Int. Ed.* **2003**, *42*, 3288.
- (8) (a) Zhao, B.; Chen, X. Y.; Cheng, P.; Liao, D. Z.; Yan, S. P.; Jiang, Z. H. *J. Am. Chem. Soc.* **2004**, *126*, 15394. (b) Zhao, B.; Gao, H. L.; Chen, X. Y.; Cheng, P.; Shi, W.; Liao, D. Z.; Yan, S. P.; Jiang, Z. H. *Chem.–Eur. J.* **2006**, *12*, 149.

Scheme 1<sup>a</sup>

<sup>a</sup> Color code: red, O; blue, N; gray, C; purple, Cr; green, Ln.

reported the first 3D Pr–Ni–Na heterotrimetallic coordination polymer based on pyridine-2,4,6-tricarboxylic acid.<sup>9</sup> While the multicarboxylate ligand iminodiacetic acid ( $H_2IDA$ ) was employed, we isolated two novel 3D 3d–4f coordination polymers  $\{[LnCr(IDA)_2(C_2O_4)]\}_n$  ( $Ln = Eu, \mathbf{1}; Sm, \mathbf{2}$ ) under hydrothermal conditions,<sup>10</sup> which were structurally characterized by X-ray single-crystal diffraction.<sup>11</sup> Both  $\mathbf{1}$  and  $\mathbf{2}$  are 3D heterometallic interpenetrating structures, in which  $H_2IDA$  ligands are found to partly break into oxalate anions (ox).

Once formed, the title compounds are stable in air and insoluble in water or in common organic solvents. In the reactions, part of the  $H_2IDA$  molecules thermally decompose into ox ligands and others coordinate with  $Cr^{III}$  ions (Scheme 1). The ox ligands link  $Ln^{III}$  ions to form one-dimensional (1D)  $\{Ln(ox)\}_n$  chains. The stability of the product and its insolubility in the reaction medium are mostly responsible for the breakage of the ligand and drive the reaction forward.

The single-crystal analysis reveals that  $\mathbf{1}$  and  $\mathbf{2}$  are isomorphous. In  $\mathbf{1}$ , the  $Cr^{III}$  ion is chelated by two IDA ligands to form a tetradentate metalloligand, with each of the uncoordinated O atoms coordinating to a  $Eu^{III}$  ion. Each  $Eu^{III}$  ion is bidentately chelated by two ox ligands. As a result, each  $Cr^{III}$  ion is six-coordinated in a distorted octahedral geometry by four O atoms and two N atoms, while each  $Eu^{III}$  ion is eight-coordinated through interactions with carboxylate groups from four metalloligands and from two ox ligands (Figure S1 in the Supporting Information). The bond lengths of Cr–N, Cr–O, and Eu–O are 2.049, 1.978, and 2.376–2.419 Å, respectively. The ox ligands link  $Eu^{III}$

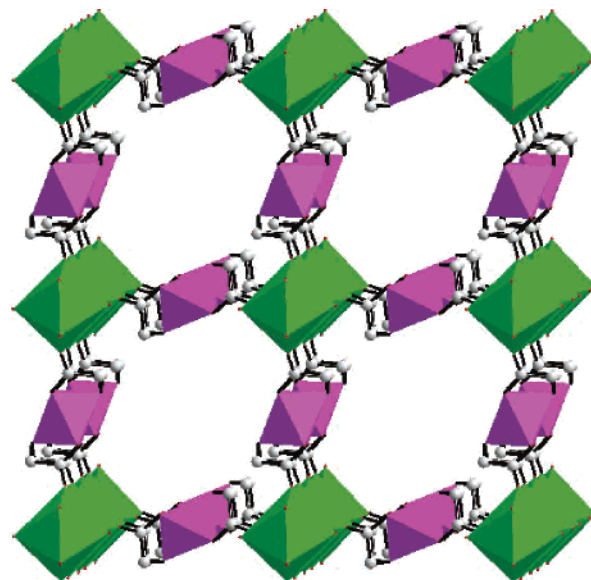


**Figure 1.** One of two interpenetrating 3D networks along the  $c$  direction. Color code: purple, Cr; green, Ln.

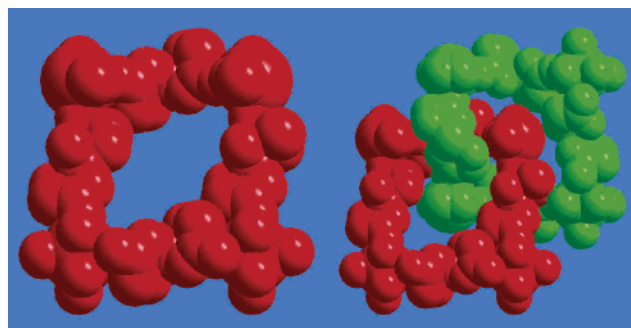


**Figure 2.** Space-filling view shows the open channel (left) and 2-fold interpenetrating networks (right) along the  $c$  direction.

ions to form  $\{Ln(ox)\}_n$  chains, which are further connected with the metalloligands to form one of two interpenetrating 3D networks (Figure 1). The shortest  $Cr \cdots Cr$ ,  $Cr \cdots Eu$ , and  $Eu \cdots Eu$  separations in  $\mathbf{1}$  are 10.799, 6.240, and 6.255 Å, respectively. Therefore, the 3D network exhibits 1D channels along the  $c$  direction with a dimensionality of  $10.8 \times 10.8 \text{ \AA}^2$  (defined by the separation between the two nearest  $Ln^{III}$  ions). To our knowledge, this is the first  $Cr^{III}$ -containing heterometallic 3D coordination polymer.

It is interesting to note that two 3D networks are interpenetrated, which results into a nonporous crystal product (Figure 2). Viewing along the  $c$  direction, each  $\{Ln(ox)\}_n$  chain in one 3D network occupies the 1D channel of another network, while each Cr center alternatively arranges for two different networks. From a topological view, each Cr and Ln center can be considered as four- and six-connected nodes, respectively. The first 3D 3d–4f interpenetrating topology is shown in Figure 3.

The phase purities of the bulk materials of  $\mathbf{1}$  and  $\mathbf{2}$  were confirmed by a comparison of their powder diffraction patterns with those calculated from the single-crystal study. Thermogravimetric analyses of the polycrystalline samples of  $\mathbf{1}$  and  $\mathbf{2}$  were performed in the temperature range 25–800 °C (Figure S2 in the Supporting Information). Both

(9) Gao, H. L.; Yi, L.; Ding, B.; Wang, H. S.; Cheng, P.; Liao, D. Z.; Yan, S. P. *Inorg. Chem.* **2006**, *45*, 481.

(10) Preparation of  $\{[LnCr(IDA)_2(C_2O_4)]\}_n$  ( $Ln = Eu, \mathbf{1}; Sm, \mathbf{2}$ ): a mixture of  $H_2IDA$  (0.6 mmol),  $Ln_2O_3$  (0.1 mmol),  $Cr(NO_3)_3 \cdot 9H_2O$  (0.2 mmol), and  $H_2O$  (20 mL) was put into a 25-mL acid digestion bomb and heated at 180 °C for 3 days. The products were collected after washing with  $H_2O$  ( $2 \times 5$  mL) and diethyl ether ( $2 \times 5$  mL). The starting pH value and the pH value after the reaction are 3 and 1.5, respectively. Yield: 57% for  $\mathbf{1}$  and 52% for  $\mathbf{2}$  (based on  $Cr^{III}$  salts). Elem. anal. Calcd for  $\mathbf{1}$ : C, 21.67; H, 1.82; N, 5.06. Found: C, 21.22; H, 2.14; N, 4.65. Elem. anal. Calcd for  $\mathbf{2}$ : C, 21.74; H, 1.82; N, 5.07. Found: C, 21.31; H, 1.65; N, 4.77.

(11) Crystal data for  $\mathbf{1}$ :  $C_{10}H_{10}CrEuN_2O_{12}$ ,  $M = 554.16$ , tetragonal,  $P4(2)/mbc$ ,  $a = 10.7990(9)$  Å,  $b = 10.7990(9)$  Å,  $c = 12.511(2)$  Å,  $V = 1459.0(3)$  Å<sup>3</sup>,  $Z = 4$ ,  $T = 294(2)$  K,  $F(000) = 1068$ , GOF = 1.048,  $R1 = 0.0211$ ,  $wR2 = 0.0598$ . Crystal data for  $\mathbf{2}$ :  $C_{10}H_{10}CrN_2O_{12}Sm$ ,  $M = 552.55$ , tetragonal,  $P4(2)/mbc$ ,  $a = 10.8168(7)$  Å,  $b = 10.8168(7)$  Å,  $c = 12.5692(17)$  Å,  $V = 1470.6(2)$  Å<sup>3</sup>,  $Z = 4$ ,  $T = 294(2)$  K,  $F(000) = 1064$ , GOF = 1.072,  $R1 = 0.0213$ ,  $wR2 = 0.0544$ . Direct methods with *SHELXS-97* and refinement on  $F^2$  using *SHELXL-97*.

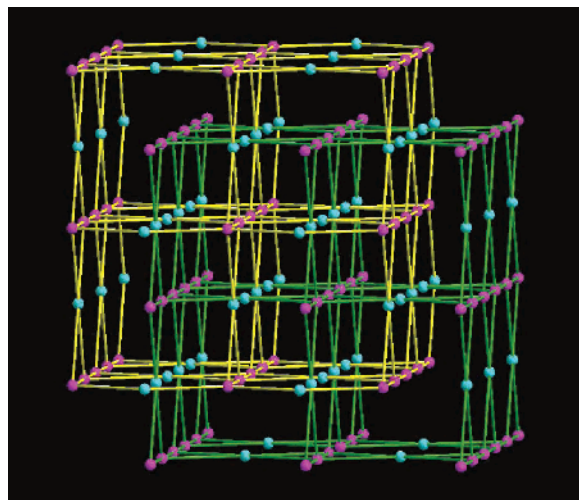


**Figure 3.** Color code: purple, Ln; cyan, Cr; yellow and green lines, connectivity between metal centers by bridged organic ligands.

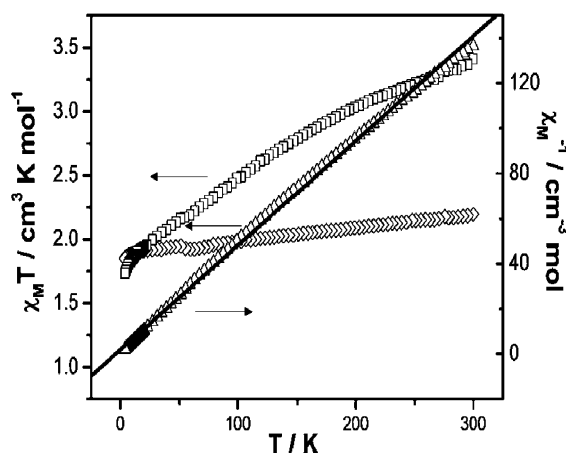


**Figure 4.** Thermal dependence of the  $\chi_M T$  and  $\chi_M^{-1}$  curves: **1** ( $\square$ ); **2** ( $\diamond$ ,  $\triangle$ ).

compounds showed high thermal stability, and the first weight loss began at 327 and 360 °C for **1** and **2**, respectively. Decomposition of the organic ligand took place up to 530 °C. After being heated to 800 °C in air, both solids were converted to black powders.

Informative magnetic susceptibility measurements of **1** and **2** have been performed on a Quantum Design MPMS-5S superconducting quantum interference device (SQUID) magnetometer in the 4–300 K temperature range, with an applied field of 1000 Oe. The diamagnetic correction was evaluated by using Pascal's constants. As shown in Figure 4, the  $\chi_M T$  value is equal to 3.41 cm<sup>3</sup> K mol<sup>-1</sup> at room temperature. The magnetic susceptibility of Eu<sup>III</sup> is expected to be zero in view of the ground state <sup>7</sup>F<sub>0</sub>, but the observed  $\chi_M T$  value of **1** is larger than the Cr<sup>III</sup>-only value. This is due to the fact that a certain amount of the magnetic moment is contributed from the excited states <sup>7</sup>F<sub>1</sub> and <sup>7</sup>F<sub>2</sub>. The  $\chi_M T$  values for **1** decrease with decreasing temperature, which attributes to the thermal depopulation of these excited levels. At 4 K, the  $\chi_M T$  value is 1.73 cm<sup>3</sup> K mol<sup>-1</sup>, which is close to the expected Cr<sup>III</sup>-only value, ca. 1.8 cm<sup>3</sup> K mol<sup>-1</sup> at 4 K.<sup>6d</sup>

For complex **2**, the observed  $\chi_M T$  value at 300 K is 2.19 cm<sup>3</sup> mol<sup>-1</sup> K, higher than the calculated value of 1.96 cm<sup>3</sup> mol<sup>-1</sup> K for one free Cr<sup>III</sup> ion and one isolated Sm<sup>III</sup> ion with a ground state of <sup>6</sup>H<sub>5/2</sub>. This may be due to the non-negligible population of excited states such as <sup>6</sup>H<sub>7/2</sub> of the Sm<sup>III</sup> ion.<sup>12</sup> Upon cooling, the  $\chi_M T$  slightly decreases and reaches 1.85 cm<sup>3</sup> mol<sup>-1</sup> K at 4 K. The linear fit via  $\chi_M = C/(T - \theta)$  reveals a Curie–Weiss behavior over 4–300 K with  $C = 2.16$  cm<sup>3</sup> mol<sup>-1</sup> K and  $\theta = -4.03$  K. The depopulation of Sm<sup>III</sup> ions from excited states, antiferromagnetic interactions between the neighboring paramagnetic centers, and/or the expected effect from a zero-field splitting of the Cr<sup>III</sup> ions may influence the magnetic behavior in this way.

Generally, Eu<sup>III</sup> and Sm<sup>III</sup> complexes exhibit a characteristic sharp luminescence.<sup>8</sup> However, the microcrystalline samples of **1** and **2** did not show obvious sharply characterized emission bands at room temperature. Because the ligand field absorption band envelope for the Cr<sup>III</sup> chromophore overlaps with the spectral range of the narrow emissions of Eu<sup>III</sup> and Sm<sup>III</sup>, the efficient quenching occurs in the Ln<sup>III</sup> luminescence, resulting from the resonance between the Ln<sup>III</sup> excited levels and the broad ligand-field state of the Cr<sup>III</sup> ion (Figure S3 in the Supporting Information).<sup>13</sup> Therefore, the maximum emission peaks at 733 nm of **1** and **2** can be attributed to <sup>2</sup>E → <sup>4</sup>A<sub>2</sub> of the Cr<sup>III</sup> ions. The peak positions and relative intensities are a little different between **1** and **2**. This quenching behavior is compared with that of other Ln–Cr complexes,<sup>6d</sup> which implies that energy transfer from Ln<sup>III</sup> to Cr<sup>III</sup> is highly effective.

In summary, the first 3D Cr-containing heterometallic coordination polymers were synthesized. The H<sub>2</sub>IDA ligands were found to partly break into ox ligands in the reaction, which connect Ln<sup>III</sup> ions to form 1D {Ln(ox)}<sub>n</sub> chains. Two 3D open networks interpenetrate each other to form the first 3D 3d–4f interpenetrating structure. The Cr<sup>III</sup>–Ln<sup>III</sup> interactions in the compounds are very weak in magnetic interactions but are strong from the viewpoint of energy transfer. The systematic and detailed investigation of magnetic and luminescent properties of Ln–Cr 3D coordination polymers is currently underway.

**Acknowledgment.** This work was supported by the National Natural Science Foundation of China (Grants 90501002 and 20425103), the NSF of Tianjin (Grant 06YFJZJC009000), and the State Key Project of Fundamental Research of MOST (Grant 2005CCA01200), People's Republic of China.

**Supporting Information Available:** X-ray crystallographic files in CIF format for **1** and **2** and additional figures (Figures S1–S6). This material is available free of charge via the Internet at <http://pubs.acs.org>.

IC060787F

(12) Andruh, M.; Bakalbassis, E.; Kahn, O.; Trombe, J. C.; Porcher, P. *Inorg. Chem.* **1993**, *32*, 1616.

(13) Brayshaw, P. A.; Buenzli, J.-C. G.; Froidevaux, P.; Harrowfield, J. M.; Kim, Y.; Sobolev, A. N. *Inorg. Chem.* **1995**, *34*, 2068.